INSTITUTE OF PLASMA PHYSICS

NAGOYA UNIVERSITY

COMPUTER SIMULATIONS ON THE NONLINEAR FREQUENCY SHIFT AND NONLINEAR MODULATION OF ION-ACOUSTIC WAVES

Yukiharu Ohsawa and Tetsuo Kamimura

IPPJ-266 November 1976

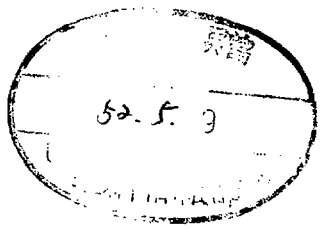

RESEARCH REPORT

NAGOYA, JAPAN

COMPUTER SIMULATIONS ON THE NONLINEAR FREQUENCY SHIFT AND NONLINEAR MODULATION OF ION-ACOUSTIC WAVES

Yukiharu Ohsawa and Tetsuo Kamimura

IPPJ-266 November 1976

Further communication about this report is to be sent to the Research Information Center, Institute of Plasma Physics, Nagoya University, Nagoya 464, Japan.

Abstract

The nonlinear behavior of ion-acoustic waves with rather short wave-length, $k\lambda_{De} \gtrsim 1$, is investigated by computer sumulations. It is observed that the nonlinear frequency shift is negative and is proportional to square root of the initial wave amplitude when the amplitude is not too large. This proportionality breaks down and the frequency shift can become positive (for large Te/Ti), when $(\tilde{n}_i/n_0)^{1/2} > 0.25$, where $\tilde{n}_i$ is the ion density perturbation and n_0 the average plasma density. Nonlinear modulation of the wave-packet is clearly seen; however, modulational instability was not observed. The importance of the effects of trapped ions to these phenomena is emphasized.

§1. Introduction

It is well known that, in the fluid description, the nonlinear behavior of an ion-acoustic wave with rather short wave-length is described by the nonlinear Schrödinger equation,

$$i\frac{\partial \phi}{\partial \tau} + p\frac{\partial^2 \phi}{\partial \xi^2} + q|\phi|^2\phi = 0 \qquad (1)$$

where $\phi(\xi,\tau)$ is the small but finite density amplitude, and τ and ξ are stretched variables in the reductive perturbation theory[1]. From eq.(1), it is apparent that the ion-acoustic wave in the fluid description is stable against modulational instabilities because the product pq is negative. Furthermore, the nonlinear frequency shift is proportional to $-q|\phi|^2$; wave-wave interactions decrease the frequency.

In a kinetic description, wave-particle resonant interactions become important. Ichikawa and Taniuti[2] have constructed a theory of nonlinear wave modulation beginning from the Vlasov equation. They assumed the contribution of particles near the phase velocity to be negligibly small in comparison with that of particles near the group velocity and hence neglected the effects of linear Landau damping and the trapped particles. Then they showed that the structure of the nonlinear Schrödinger equation (1) is modified in that a nonlocal nonlinear term is added to eq.(1) and the sign of the local nonlinear coupling coefficient q is reversed. They conluded that the ion-acoustic wave does become unstable with respect to the modulational instability.

Although this theory neglected the effects of trapped particles, several recent experiments have shown their importance. Sugai et al.[3] reported that the nonlinear frequency shift is negative and is proportional to the square root of the initial amplitude. Their results imply that the frequency shift is mainly due to trapped ions[4]. Ikezi and Schwarzenegger[5] observed experimentally that the nonlinear frequency shift is much larger than that obtained from the fluid description, i.e., from eq.(1), and that the ion-acoustic wave is modulationally stable. They emphasize the importance of the phase velocity shift due to trapped ions. Both experiments were performed in the parameter region $10 \lesssim T_e/T_i \lesssim 30$ and $k/k_{De} \sim 1$, where T_e, T_i, k_{De} and k are the electron and ion temperatures, the electron Debye wave-number, and the wave-number of the ion-acoustic wave, respectively. These experimental results suggest that the effects of trapped particles should be included when one considers the evolution of the ion-acoustic wave with $k/k_{De} \lesssim 1$ and $10 \lesssim T_e/T_i \lesssim 30$.

The purpose of our computer simulations is to investigate the evolution of the nonlinear ion-acoustic wave with a rather short wave-length, $\lambda \lesssim 2\pi\lambda_{De}$ where λ_{De} is the electron Debye length. We pay special attention to the nonlinear frequency shift due to trapped ions and to the evolution of the wave-packet, whose envelope varies slowly in space.

In §2, the model for the computer simulations is described. In §3, the nonlinear frequency shift of the ion-acoustic wave is studied. It is found to be proportional to the square root of the initial wave amplitude ε when ε is

small. This implies that the frequency shift is mainly caused by the trapped particles. But when ε becomes large, this proportionality breaks down. §4 describes the space-time evolution of the wave-packet. It is shown that in the rising part of the envelope, the wave-number decreases, while in the falling part it increases. The modulational instability was not observed at all. Our conclusions are summarized in §5.

§2. Model for the Computer Simulations

We consider a one-dimensional, electro-static problem. The electrons are assumed to be in a Boltzmann distribution with constant temperature. For the ions, a hybrid solution algorithm is used, which was originated by Denavit.[6] In this model, the two-dimensional (x,v) phase space is covered with a rectangular grid. Initially, all simulation particles are located on the grid points, with mass and charge at location (x_j, v_j) proportional to the initial value of the distribution function $f(x_j,v_j)$. The particles move along the characteristics of the Vlasov equation, and at a later time the distribution function, f(x,y), is calculated from the locations and masses of the simulation particles. The CIC(Cloud in Cell) model[7] is used for the simulation particles. Then, apart from numerical errors, our computations are equivalent to solving the following set of equations:

$$\frac{\partial f}{\partial t} + v\frac{\partial f}{\partial x} + \frac{eE}{M}\frac{\partial f}{\partial v} = 0 \qquad (2)$$

$$n_e/n_0 = \exp(e\psi/T_e) \quad , \qquad (3)$$

$$-\partial^2\psi/\partial x^2 = 4\pi e(n_i - n_e) \quad , \qquad (4)$$

$$E = -\partial\psi/\partial x \quad . \qquad (5)$$

Here n_0, n_e, n_i and ψ are the average plasma density, the electron and ion densities and the electric potential, respectively. Equation (2) is the Vlasov equation for the ion distribution function. Combining eqs.(3), (4), and (5), we obtain the equation for the electric field

$$E = -\frac{T_e}{e}\frac{\partial}{\partial x}\left[\ln\left(n_i - \frac{1}{4\pi e}\frac{\partial E}{\partial x}\right)\right] \quad . \qquad (6)$$

The ion density n_i is given by integrating the distribution function f over velocity space. Then, we can obtain the electric field by using the implicit iteration scheme.[8] Periodic boundary conditions are used. The total conserved energy for our model is

$$E_{tot} = \frac{M}{2}\int_L dx\int_{-\infty}^{\infty} dv f v^2 + \frac{1}{8\pi}\int_L dx E^2 + \int_L dx n_e e\psi + \text{const.} \quad , \qquad (7)$$

where L is the total length of the test area. Equation (7) has the same form as eq.(8) in Ref. 9.

In our model, the velocity distribution of the particles is replaced by a set of discrete beams. Such a system is known to be subject to the beaming instability, even if the

envelope of the beam density is Maxwellian[6),10)]. The dispersion relation for the beaming instability in a system composed of multi-electron beams which pass through a uniform neutralizing background of positive immobile ions was obtained by Dawson[10)]. In our model, which consists of multi-ion beams with Maxwellian envelope and an electron fluid, the dispersion relation for the beaming instability is obtained in a similar mannar. As in Ref. 10, the growth rate here is also given, in the limit of $\Delta v \to 0$, by

$$\gamma \simeq (k\Delta v/2\pi)\,|\ln(\Delta v/v_T)|$$

where v_T and Δv are the ion thermal velocity and the velocity interval of the beams. In order to prevent the beaming instability from growing, we reconstruct the distribution function every N time steps during the course of the simulation run[6)]. The time intervals between reconstructions are taken to be short compared to the inverse of the maximum growth rate of the beaming instability. In our simulations we take N to be usually 10.

The ion-acoustic wave is excited with an initial ion distribution function given by

$$f(x,v) = (n_0/\sqrt{2\pi}\, v_T)\{1+[1-\varepsilon_m\cos(k_m x)]\varepsilon\cos(kx)\}$$

$$\times \exp\{-[v-(1-\varepsilon_m\cos(k_m x))\varepsilon v_p\cos(kx)]^2/2v_T^2\}, \qquad (8)$$

where ε, ε_m and k_m are the perturbed ion density normalized by

n_0, the amplitude of the modulation, and the wave-number of the modulation, respectively. To the phase velocity, v_p, of the ion-acoustic wave, we gave the approximate value $v_p^2 = (T_e/M)\{3T_i/T_e + 1/(k^2\lambda_{De}^2 + 1)\}$. At the time when the monochromatic wave is excited, ε_m is taken to be zero. It was observed that the distribution function of eq.(8) excites a backward wave as well as a forward one. The amplitude of the backward wave is, however, small in comparison with that of the forward wave, the ratio of their amplitudes being about 0.1. In our simulations, the distribution function has a finite value in the velocity region $-5v_T \lesssim v \lesssim 8\ v_T$. Outside of this region, it is zero. The velocity interval Δv is taken to be $180 \lesssim 13v_T/\Delta v \lesssim 280$. The spatial mesh size Δx is $64 \lesssim L/\Delta x \lesssim 256$, with L being the total system length. The time step Δt is chosen to be $\omega_{pi}\Delta t = 0.2$.

When the wave amplitude ε is small, the dispersion relation of the ion-acoustic wave thus excited is in good agreement with that of Langdon's theory[7]. This is shown in Fig.(1).

§3. Nonlinear Frequency Shift

In this section, the nonlinear frequency shift of the ion-acoustic wave is studied. In this paper, the nonlinaer frequency shift is defined by

$$\delta\omega_r = \omega_{rNL} - \omega_{rL}$$

where ω_{rNL} and ω_{rL} are the real part of the frequency of the nonlinear wave and of the linear wave, respectively. If the frequency shift is caused by wave-wave interactions, its shift is known to be proportional to the square of the wave amplitude[1]. On the other hand, if the shift is mainly due to trapped particles, the shift may be proportional to the square root of the initial wave amplitude. For the electron wave, this has been pointed out theoretically[4] and is supported from computer simulations[11]. For the ion-acoustic wave, direct application of the theory in Ref.4 leads to a similar result, i.e. $\delta\omega_r \propto \sqrt{\varepsilon}$, when the effects of the trapped particles are taken into account. And, Sugai et al. have observed experimentally that the frequency shift $\delta\omega_r$ of the ion-acoustic wave is indeed proportional to the square root of the initial amplitude.

In Fig.(2), the observed frequency shift of the plane wave is plotted as a function of the square root of the initial wave amplitude. Wave excitation is achieved by the distribution function of eq.(8) with $\varepsilon_m=0$. The frequency of the wave is known from temporal variation of the phase of a given wave-number k. Provided the wave with wave-number k has frequency ω_k, the density perturbation of the k-th mode takes the following form,

$$n_{ik}(t) = h\{\cos(-\omega_k t + \delta)\cos(kx) - \sin(-\omega_k t + \delta)\sin(kx)\}, \quad (9)$$

where h and δ are constants. In the computer simulations, we can measure the coefficients of cos(kx) and sin(kx) by the

Fourier transformation of the ion density. Then, by virtue of eq.(9), we obtain, from the temporal variation of coefficients of cos(kx) and sin(kx), the frequency of a given wave-number k. We can see from Fig.(2) that, except for the case of $T_e/T_i=30$ and $\sqrt{\varepsilon}\gtrsim 0.35$, the frequency shift is negative. Its magnitude increases as T_e/T_i decreases. The shift is proportional to the square root of the amplitude when $\sqrt{\varepsilon}\lesssim 0.3$, which therefore indicates that the frequency shift is caused by trapped ions. It is interesting to note that the amplitude dependence of the frequency shift seems to change when $\sqrt{\varepsilon}\gtrsim 0.3$; the rate of increase in $|\delta\omega_r|$ then becomes smaller. For the case of $T_e/T_i=30$, the frequency shift stops increasing when $\sqrt{\varepsilon}\gtrsim 0.25$. Furthermore, for $\sqrt{\varepsilon}\gtrsim 0.35$, the frequency shift becomes positive; i.e., the frequency of the nonlinear ion-acoustic wave becomes larger than that of the linear wave. Quite recently, Kim[12] showed theoretically that, for the electron wave, the nonlinear frequency shift can become positive at large amplitudes. If we apply this theory to the ion-acoustic wave, we find that the frequency shift becomes positive when v_p/v_T and α are large, with $\alpha = (v_p/v_T)\{(T_e/T_i)\varepsilon/(1 + k^2\lambda^2_{De})\}^{1/2}$, and also that $\delta\omega_r$ strongly depends on α while its dependence on v_p/v_T is rather weak. For $T_e/T_i \gg 1$ and $k^2\lambda^2_{De}\sim 1$, we see that $v_p/v_T \sim \sqrt{T_e/T_i}$ and $\alpha \sim (T_e/T_i)$. Hence, the dependence of $\delta\omega_r$ on T_e/T_i is very strong, which is clearly shown in Fig.(2).

When ε_m has a nonzero value, the intial distribution function of eq.(8) excites a modulated ion-acoustic wave. The amplitude dependence of the frequency shift of such a modulated

wave is shown in Fig.(3), for the case where $\varepsilon_m = 1.0$ and $k_m/k = 0.1$, with other parameters the same as in Fig.(2). When $\varepsilon_m = 1.0$, the amplitude at the top of the envelope is $2\mathcal{E}$. Hence the horizontal axis in Fig.(3) is measured by the value of $(2\varepsilon)^{1/2}$. Although now there are reflected ions as well as trapped ions, no drastic change from the case of the plane wave is seen. Namely, the magnitude of the frequency shift still increases as T_e/T_i decreases, and the shift is proportional to the square root of the amplitude when $\sqrt{\varepsilon} \lesssim 0.3$. Hence, even in the case of a wave-packet with spatially (slowly) varying invelope, the nonlinear frequency shift is mainly caused by the trapped particles.

Before closing this section, we note the following. From the temporal variation of the wave-amplitude, which is not presented in this paper, we did observe that as the initial amplitude increases, the initial damping rate of the ion-acoustic wave increases. We also found that, when the initial amplitude is not so small, the period of the amplitude oscillation is longer than that given by the following equation

$$T_{os} = 2\pi/(eE_0\, k/M)^{1/2} \quad ,$$

where E_0 is the amplitude of the electric field. These intersting phenomena will be discussed elsewhere in a later paper.

§4. Evolution of the Wave-Packet

In this section, the time evolution of the ion-acoustic wave packet is studied. The nonlinear Schrödinger equation derived from the fluid equations contains wave-wave interations but,of course, wave-particle resonant interations are not included. The wave-particle resonant interations have been taken into account in the modified nonlinear Schrödinger equation obtained by Ichikawa and Taniuti[2]. But in their theory, the effects of the trapped particles are neglected, because they considered the case where contribution from particles near the group velocity are more important than those from particles near the phase velocity. However, the real experiments[3),5)] already cited and the results of the previous section indicate that, in the region $k/k_{De} \tilde{<} 1$ and $10 \tilde{<} T_e/T_i \tilde{<} 30$, the nonlinear effects are mainly due to trapped ions. The following computations on the evolution of the wave-packet were done in the same parameter region, and hence the effect of trapped ions on the evolution are expected to be significant.

In Fig.(4), the time evolution of the wave-packet is depicted. The profiles are plotted in the frame moving with velocity v_p (relative to the laboratory frame). Excitation of the wave is achieved by the initial ion distribution function of eq.(8): The parameters are taken to be $\varepsilon=0.1$, $\varepsilon_m=1.0$, $k_m/k_{De}=0.1$, $k/k_{De}=1.0$, and $T_e/T_i=20$. For smaller amplitude waves ($\varepsilon \sim 0.005$), which are not shown in Fig.(4),

the wave-packet expands due to dispersion and damps by Landau damping. But, for the larger amplitude wave which is shown in Fig.(4), the wave-number of the carrier wave is modulated as the wave propagates, and the envelope considerably changes its shape. The initial ion density profile is plotted in Fig.(4a). At time $\omega_{pi}t=10$, the maximum point of the envelope is seen to have moved slightly backward. At $\omega_{pi}t=15$, wave-number modulation of the carrier wave is observed. In the rising part of the envelope, the wave-number decreases, whereas in the falling part, it increases. The top of the envelope is flattened. For the plane wave with $\varepsilon\approx 0.16$, the amplitude damps rapidly (more rapidly than the Landau damping rate) till $\omega_{pi}t=15\sim 20$, then it begins to oscillate. Observed time period of the amplitude oscillation is about $\omega_{pi}T_{os}\approx 50$. In view of these results of the plane wave, we may interpret that the flattening of the envelope at $\omega_{pi}t=15$ is caused by the amplitude oscillation of the larger amplitude part. At $\omega_{pi}t=30$, expansion of the wave-packet due to group velocity dispersion is observed. The maximum point of the envelope has moved forward. At $\omega_{pi}t=50$, a long wave-lengh density perturbation appears. Its lengh is on about the same scale as that of the wave-packet. Figures(4f),(4g) and (4h) then show the density profiles at $\omega_{pi}t=60,85$ and 105. In these latter three figures, the local wave-number of the carrier wave is not the same at all spatial points. A smaller wave-number corresponds to the rising part of the envelope in the initial stage, and a larger wave-number corresponds to the falling part of the envelope in the initial

stage. We see that the amplitude of the carrier wave is rather uniform in space. The long wave-length perturbation is clearly seen.

Figure(5) shows the temporal evolution of the Fourier amplitudes of the wave corresponding to Fig.(4). Because the excited wave is modulated, there are three modes in k-space at $\omega_{pi}t=0$. One is the carrier wave, and the other two are sidebands. For the smaller amplitude wave, i.e., with $\varepsilon=0.005$, the Fourier amplitudes damp in time, but the relative magnitude of the Fourier amplitudes does not change drastically. On the other hand, for the larger amplitude wave, with $\varepsilon=0.1$, the sidebands grow and the carrier damps as the wave propagates. This corresponds to the wave-number modulation of Fig.(4).

Finally, we have carried out simulations with various sets of values for ε_m, k_m, T_e/T_i and ε. The modulational instability was never observed.

We wish to point out that these fertures of ion wave evolution observed in our simulations are very similar to those observed in the experiments by Ikezi and Schwarzenegger.[5] On the basis of a phenomenological equation [their eq.(4)] they give an interesting physical interpretation of the wave evolution and claim that the nonlinear frequency shift due to trapped ions can give rise to a wave-number modulation such that the wave-number decreases during the rising part of the envelope while it increases during the falling part. Then, if their phenominological equation is valid, in view of our result in the previous section that the frequency shift is negative for

$T_e/T_i \simeq 20$ and is due to the trapped ions, may conclude that also the wave-number modulation is mainly caused by trapped ions.

§5, Conclusions

The nonlinear behavior of ion-acoustic waves with short wave-length was investigated by computer simulations. We paid special attention to the effects of trapped ions from among other nonlinear effects. The temperature ratio T_e/T_i was taken to be in the range $15 \lesssim T_e/T_i \lesssim 30$. The nonlinear frequency shift of the ion-acoustic wave is negative and is shown to be proportional to the square root of the initial amplitude ε when $\varepsilon \lesssim 0.1$. This fact indicates that the frequency shift is mainly caused by trapped ions. We also note that this amplitude dependence of the frequency shift changes when $\varepsilon \gtrsim 0.1$; the increase of the frequency shift then becomes slower. In particular, for $T_e/T_i=30$, the frequency shift becomes positive when $\varepsilon \gtrsim 0.1$. Bearing in mind these results, we next examined the behavior of a wave-packet including the effects of trapped particles. Simulations for the evolution of the wave-packet clearly show the nonlinear modulation of the ion-acoustic wave. In the rising part of the envelope, the wave-number decreases, whereas in the falling part, it increases. In correspondence with the wave-number modulation, the sidebands grow and the carrier damps. The modulational instability was never observed.

Acknowledgements

The authors wish to thank Professor T. Taniuti, Professor H. Ikezi and Professor Y. Midzuno for helpful discussions. They are also grateful to Dr. VanDam for his critical reading of this manuscript and to the members of the computer center of the Institute of Plasma Physics, Nagoya University, for their assistence with the computer simulations.

References

1) K. Shimizu and Y.H. Ichikawa: J. Phys. Soc. Japan 33 (1972) 789.

2) Y.H. Ichikawa and T. Taniuti: J. Phys. Soc. Japan 34 (1973) 513.

3) H. Sugai, R. Hatakeyama, K. Saeki and M. Inutake: Phys Fluids, to be published.

4) G. J. Morales and T. M. O'Neil: Phys. Rev. Lett. 28 (1972) 417; W. M. Manheimer and R. W. Flynn: Phys. Fluids 14 (1971) 2393.

5) H. Ikezi and K. Schwarzenegger: submitted to Phys. Rev. Lett.

6) J. Denavit: J. Computational Phys. 9 (1972) 75.

7) A. B. Langdon: J. Comput. Phys. 6 (1970) 247.

8) P. H. Sakanaka, C. K. Chu and T. C. Marshall: Phys. Fluids 14 (1971) 611.

9) R. J. Mason: Phys. Fluids 14 (1971) 1934.

10) J. M. Dawson: Phys. Rev. 118 (1960) 381.

11) A. Lee and G. Pocobelli: Phys. Fluids 16 (1973) 1964; Y. Matsuda and F. W. Crawford: Phys. Fluids 18 (1975) 1336; J. M. Canosa: IBM Palo Alto Scientific Center Report No. G320-3343 (1975).

12) H. Kim: Phys. Fluids 19 (1976) 1362.

Figure Captions

Fig.1. Linear dispersion relation for ion-acoustic waves with $T_e/T_i=20$. The solid lines are obtained from Langdon's theory. Triangles and circls denote the observed values of ω_r/ω_{pi} and ω_i/ω_{pi}, where ω_r and ω_i are the real and imaginary parts of the frequency. The mesh size in phase space in given by $L/(2\pi/k)=2$, $L/\Delta x=64$, and $13v_T/\Delta v=183$.

Fig.2. Nonlinear frequency shift of the nonochromatic ion-acoustic wave. The observed shift, $-\delta\omega_r/\omega_{rL}$, is plotted as a function of the amplitude $\sqrt{\varepsilon}$. The wave-number is chosen to be $k/k_{De}=1.0$. The marks of cross are the values from the real experiment of Sugai et al. with $k/k_{De}=0.4$ and $T_e/T_i=10$. The mesh size is taken to be $L/(2\pi/k)=2$, $L/\Delta x=64$, $13v_T/\Delta v=183$. (We also tested with $13v_T/\Delta v=1090$, but the results were almost the same.)

Fig.3. Nonlinear frequency shift of the modulated ion-acoustic wave as a function of $(2\varepsilon)^{1/2}$ with $k/k_{De}=1.0$, $k_m/k=0.1$, and $\varepsilon_m=1.0$. Here $L/(2\pi/k)=10$, $L/\Delta x=256$, and $13v_T/\Delta v=290$.

Fig.4. Evolution of the wave-packet with $T_e/T_i=20$, $\varepsilon=0.1$, and $k/k_{De}=1.0$. The ion density profiles are plotted in the wave frame. (In the laboratory frame, the wave propagates to the right.) $L/(2\pi/k)=10$, $L/\Delta x=256$, and $13v_T/\Delta v=290$.

Fig.5. Temporal behavior of the Fourier amplitudes of the ion density perturbation. The horizontal axis is the wave-number $kL/2\pi$, which assumes integer values since the system is spatially periodic with period L. Parameters are the same as those in Fig.4.

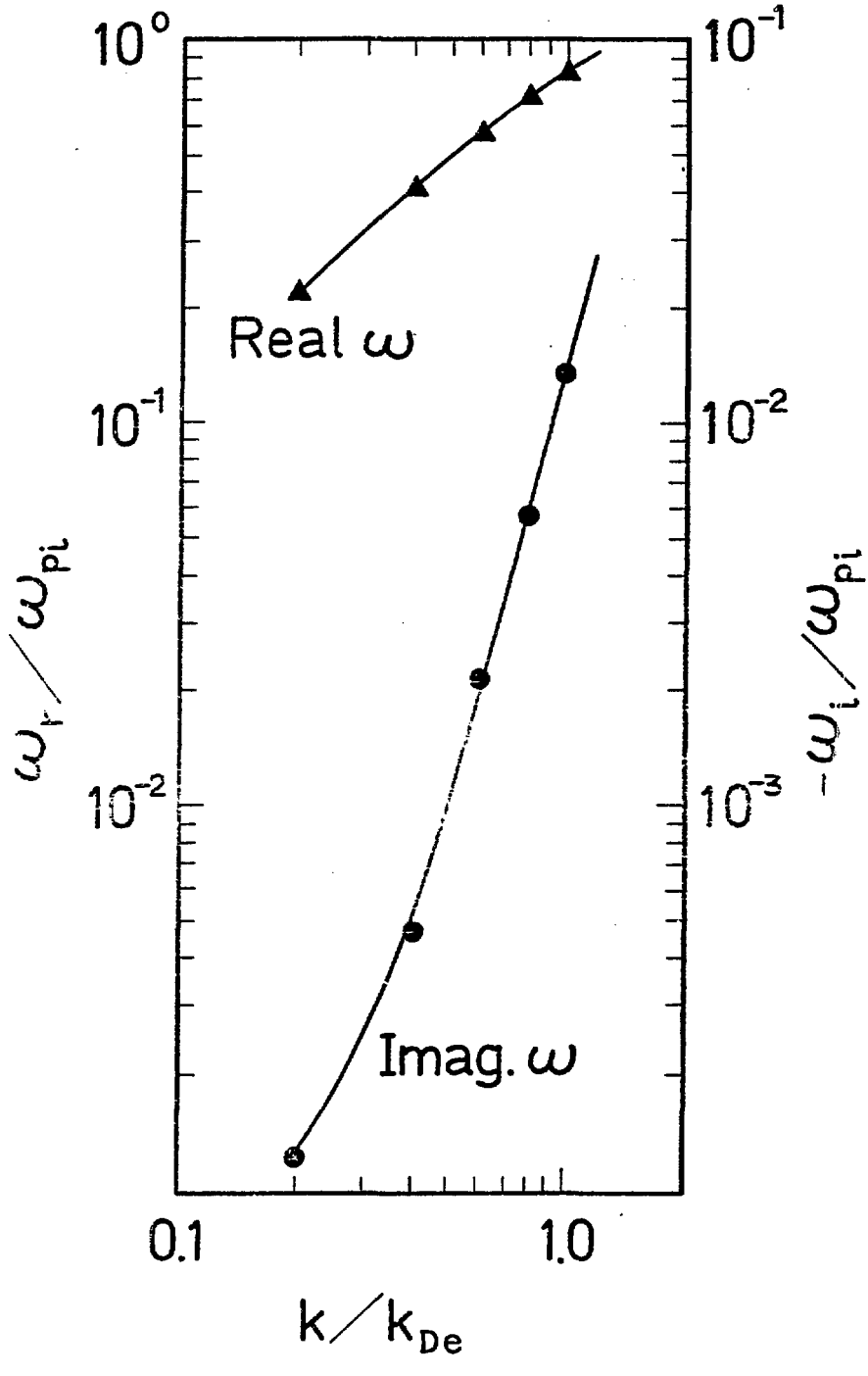
10^0
10^{-1}
10^{-1}
10^{-2}
10^{-2}
10^{-3}
Real ω
Imag. ω
ω_r / ω_{Pi}
$-\omega_i / \omega_{Pi}$
0.1
1.0
k / k_{De}

Fig. 1

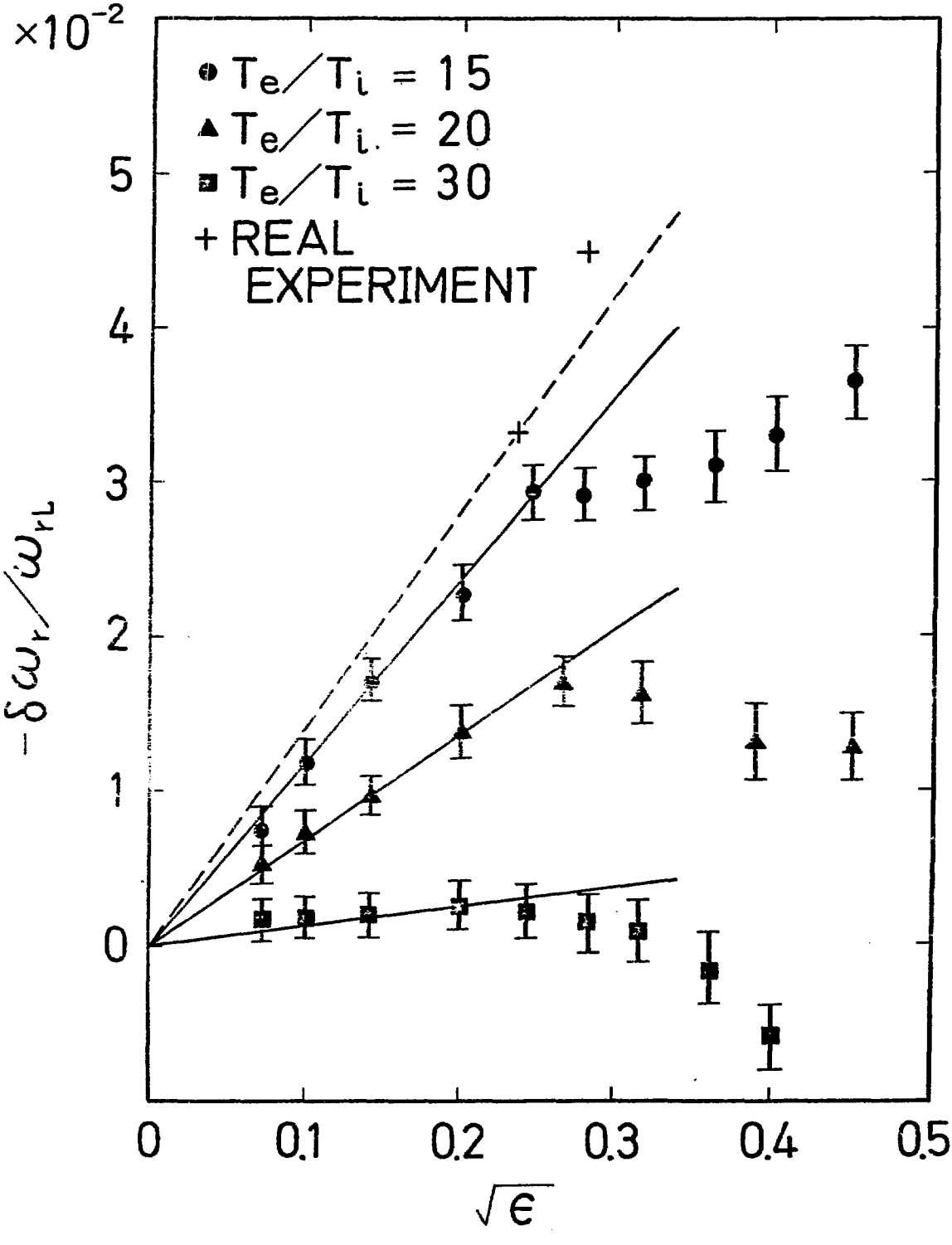
×10⁻²
Te/Ti = 15
Te/Ti = 20
Te/Ti = 30
+ REAL EXPERIMENT
5
4
3
2
1
0
0
0.1
0.2
0.3
0.4
0.5
√ε
−δω_r/ω_rL

Fig. 2

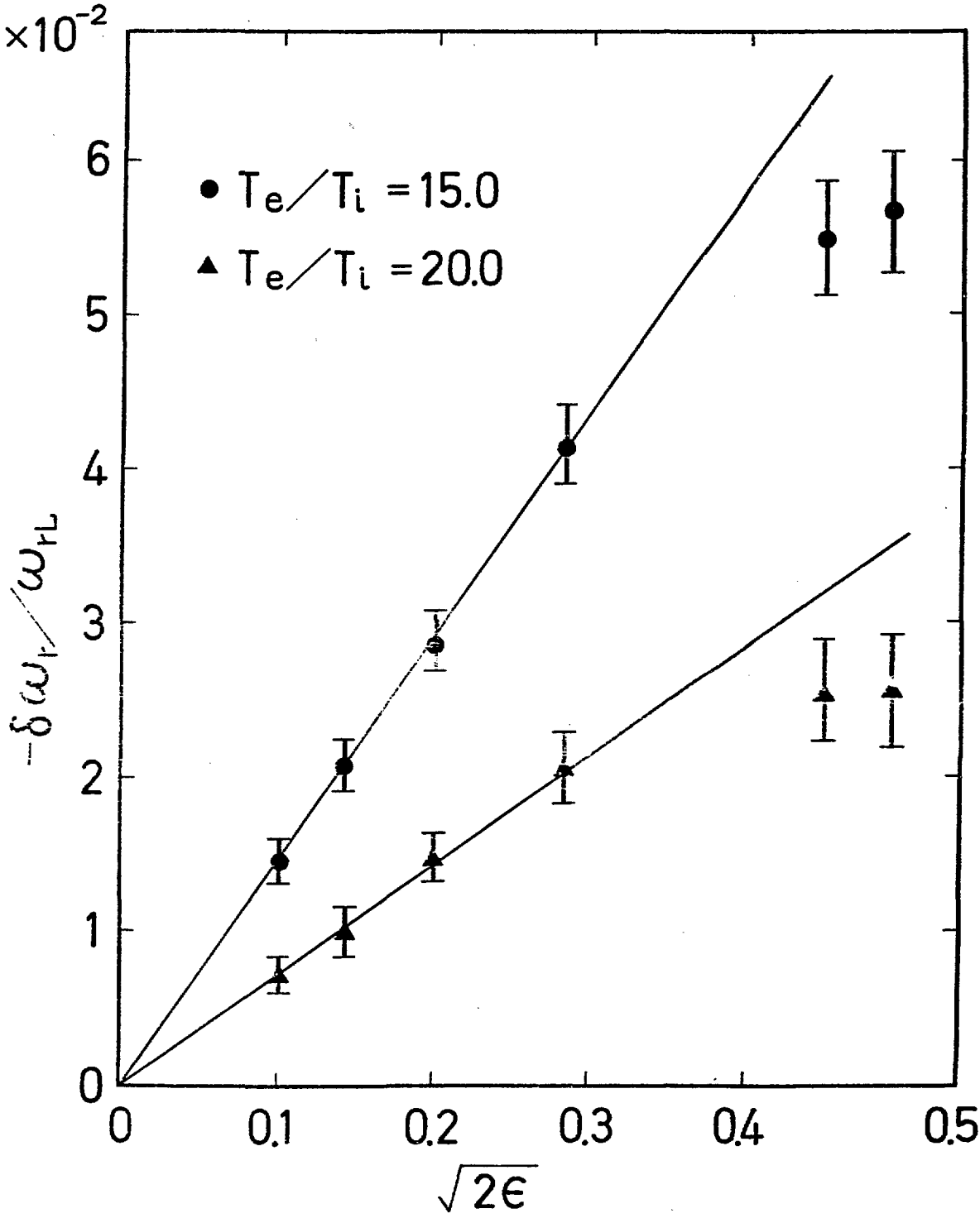

Fig. 3

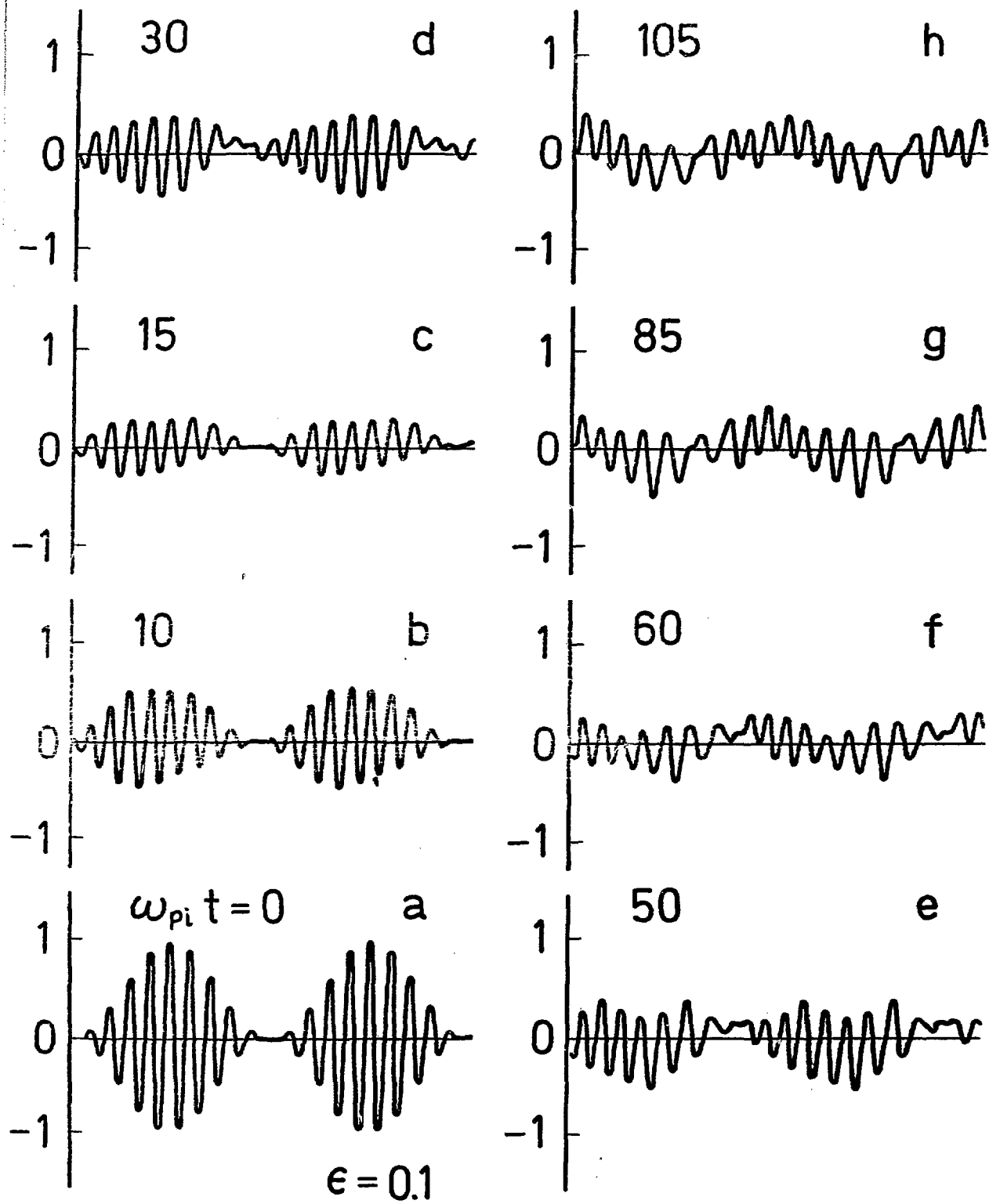

Fig. 4

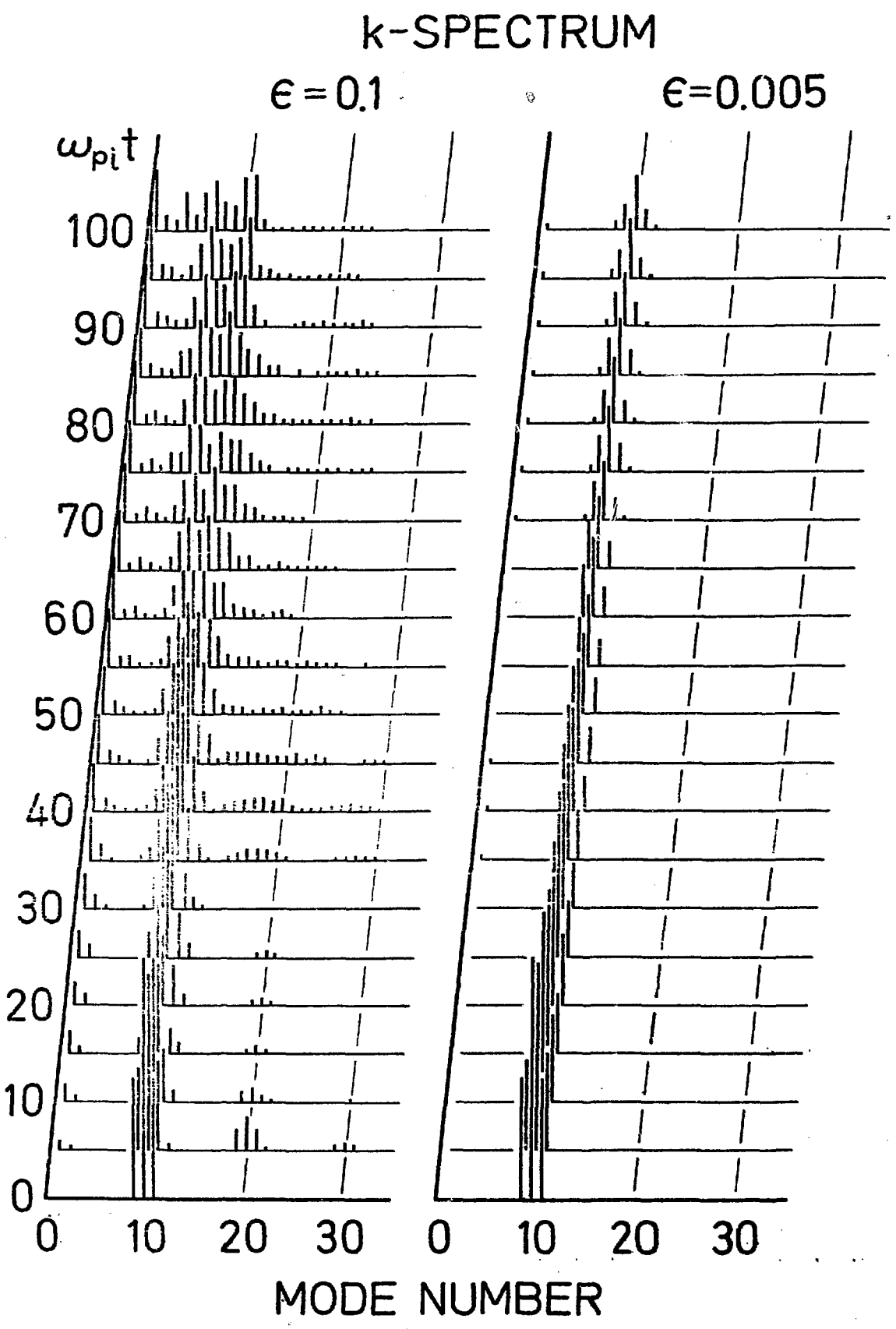
k-SPECTRUM
ϵ = 0.1
ϵ=0.005
ωpit
100
90
80
70
60
50
40
30
20
10
0
0
10
20
30
0
10
20
30
MODE NUMBER

Fig. 5